

Bronchial region extraction from 3D chest CT image by voxel classification based on local intensity structure

T. Kitasaka¹ *, H. Yano², M. Feuerstein³, and K. Mori^{2,4}

¹ School of Information Science, Aichi Institute of Technology,
kitasaka@aitech.ac.jp,

² Graduate School of Information Science, Nagoya University, Japan,

³ Computer Aided Medical Procedures (CAMP), Technische Universitat Munchen,
Germany,

⁴ Information and Communications Headquarters, Nagoya University, Japan.

Abstract. This paper presents a method for extracting bronchial regions from 3D chest CT images by voxel classification based on local intensity structure. Most of previous methods are based on trace of bronchial tree structures by region growing algorithms, so that it fails when the bronchial lumen is interrupted by abnormalities such as tumor. Thus, we focus on detecting candidate voxels which have bronchus-like intensity structure and selecting appropriate candidates from them, instead of tracing the bronchial tree, into bronchial region extraction. Two types of tube enhancement filters are employed in our algorithm. One is designed to enhance bronchus-like intensity structure where low intensity regions are surrounded by higher intensity regions and cross section of a bronchus along its running direction forms the circular shape. The other filter is utilized to enhance line structures based on the Hessian matrix analysis. The experimental results for eight cases of 3D chest CT images showed that the accuracy of the proposed method improved by 10 % compared with a previous method, while FPs increased relatively.

1 Introduction

In diagnosis and treatment of chest diseases, precise recognition of the bronchus is important. Lung cancer and chronic obstructive pulmonary disease (COPD) are representative diseases in the chest. These diseases strongly correlate or affect bronchial morphology. In clinical practice, 3D chest X-ray CT images are used for inspection for such diseases, since the bronchus is clearly depicted in

* The authors thank our colleagues for suggestions and advices. Parts of this research were supported by the Grant-In-Aid for Scientific Research from the Ministry of Education (MEXT), Japan Society for the Promotion of Science (JSPS), the Japan Society for Promotion of Science, and the Grant-In-Aid for Cancer Research from the Ministry of Health and Welfare. The authors also thank to Dr. Hiroshi Natori, Dr. Masaki Mori, Dr. Hirotsugu Takabatake, and Dr. Yoshinori Hasegawa for their medical advices.

comparison with any other medical imaging devices. Therefore, a computer aided diagnosis or treatment system of the chest should recognize bronchial structure before measuring precise features of suspicious regions from chest CT images. Many studies on bronchus recognition for automated detection and analysis of suspicious regions observed in the bronchus or lung have been reported [1–11].

Mori et al. [1], Kitasaka et al. [2], Feuerstein et al. [3], Tschirren et al. [4], Schlathoelter et al. [5], Lo et al. [6] uses region growing or front propagation methods to segment and restructure a bronchial region. There are two main issues of the methods based on region growing algorithms; (a) leakage issue and (b) interruption of growing. First, leakages beyond the bronchial wall occur at the areas where intensity contrast between the bronchial wall and bronchial lumen becomes low, e.g. due to the partial volume effect. Second, when there is interruption such as a tumor or intensity gap caused by heart beat, bronchial regions beyond them cannot be extracted at all. Contrastly, the methods based on classification that distinguishes voxels in the bronchus from those in others using several bronchial features [8–11]. These methods use typical features of the bronchus, such as (a) low intensity at the bronchial lumen, (b) relatively higher intensity at the bronchial wall than that of bronchial lumen, (c) the bronchus forms tube structure, and (d) the radius of a bronchial branch do not change rapidly along its running direction. Lo et al. [11] introduced a method for extracting bronchial regions from CT volume based on voxel classification approach. In this method voxels of an input CT volume are classified into airway voxels or others based on an airway appearance model. Then, false positives (FPs) are removed by using the measure of vessel orientation similarity. We also propose a novel method based on bronchial feature classification by developing features of bronchial tube structure in order to cope with the second issue described above. Our method focuses on development of new bronchial feature as a preceding step of utilization of a statistical bronchial atlas such as an airway appearance model Lo et al. used.

We explain our features and processing procedures in 2, conduct the experiment in 3 and add discussion in 4.

2 Method

2.1 Overview

We utilize the following image features of bronchi that can be seen on CT images: (1) low intensity in luminal area, (2) relatively higher intensity in the bronchial wall region than that in luminal area, and (3) tube-like structure. Thus, we extract bronchial regions by classifying each voxel based on above features. In the preprocessing step, we apply a LoG filter to an input CT volume to enhance bronchial wall edges. Then, two types of tube enhancement filters are employed to detect voxels showing bronchus-like structures. The first filter enhances voxels forming line structures based on the Hessian analysis [12]. The second filter enhances voxels having bronchus-like intensity structure that (a) low intensity lumen is surrounded by higher intensity wall and (b) a cross section of a bronchus

along its running direction forms the circular shape. Then, we detect candidate voxels of bronchus regions based on outputs of above two filters. Since the above procedure extracts only voxels around center of bronchus regions, bronchus regions are extracted by the postprocessing step that recovers bronchus regions.

2.2 Preprocessing

We apply a LoG filter of standard deviation σ to sharpen an input volume. Let \mathbf{F} and \mathbf{G} be the input and output images. A LoG filter with σ is represented by LoG_σ . Our sharpening operation can be expressed as

$$\mathbf{G} = \mathbf{F} - wLoG_\sigma(\mathbf{F}), \quad (1)$$

where w is a weight to control the effect of sharpening operation. Bronchial walls, especially bronchial walls of thinner bronchial branches, are enhanced with suppressing noise.

2.3 Line enhancement filter

We enhance luminal region of bronchi by performing the Hessian matrix analysis method proposed in [12]. From eigenvalues of the Hessian matrix computed for each voxel, λ_1 , λ_2 and λ_3 ($\lambda_1 \leq \lambda_2 \leq \lambda_3$), a liness measure $S_{\sigma_h}^{line}(\lambda_1, \lambda_2, \lambda_3)$ for scale σ_h is calculated by

$$S_{\sigma_h}^{line}(\lambda_1, \lambda_2, \lambda_3) = \begin{cases} |\lambda_3| \cdot \psi(\lambda_2; \lambda_3) \cdot \omega(\lambda_1; \lambda_2) & (\lambda_3 \geq \lambda_2 > 0) \\ 0 & otherwise \end{cases} \quad (2)$$

where

$$\psi(\lambda_s, \lambda_t) = \begin{cases} (\frac{\lambda_s}{\lambda_t})^\gamma & (\lambda_t \geq \lambda_s > 0) \\ 0 & otherwise \end{cases} \quad (3)$$

and

$$\omega(\lambda_s, \lambda_t) = \begin{cases} (1 + \frac{\lambda_s}{|\lambda_t|})^\gamma & (\lambda_t \geq \lambda_s > 0) \\ (1 - \alpha \frac{\lambda_s}{|\lambda_t|})^\gamma & (-\frac{\lambda_t}{\alpha} < \lambda_s < 0) \\ 0 & otherwise \end{cases} \quad (4)$$

$S_{\sigma_h}^{line}$ is calculated by changing scale σ_h . Output of each voxel \mathbf{p} by this filter, $l_h(\mathbf{p})$, is the largest response at certain σ_h . Figure 1 shows examples of outputs of the line enhancement filter with and without the preprocessing. Thinner bronchial vessels are well enhanced by performing the preprocessing as shown in the left figure. However, other structures are enhanced as well. We extract bronchial candidate voxels satisfying $l_h(\mathbf{p}) > T_l$. For an extracted voxel \mathbf{p} , we calculate the running direction \mathbf{c} and radius R of the bronchial branch to which the voxel \mathbf{p} belongs as the eigen vector \mathbf{e}_1 corresponding to λ_1 and $4\sigma_h$, respectively.

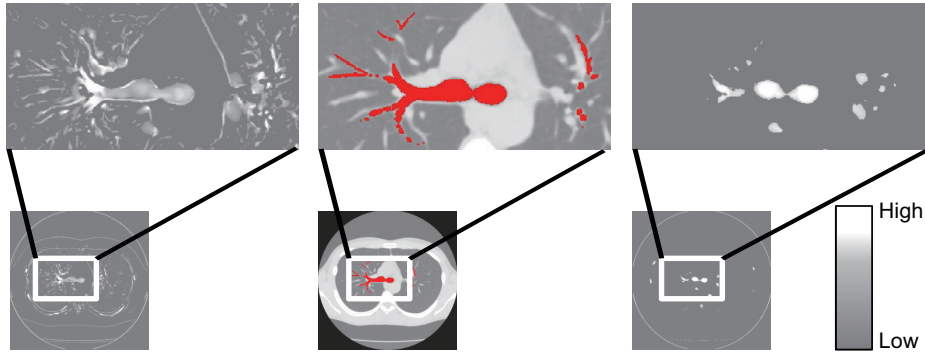


Fig. 1. Examples of line enhancement filter w and w/o LoG filter. (left) Result with LoG filter, (middle) bronchus region manually inputted in red overlaid on a CT slice and (right) result without LoG filter. Thinner bronchial vessels are well enhanced in the left figure compared with the right figure, while other structures are enhanced as well.

2.4 Tube extraction filter

To extract voxels having bronchus-like intensity structure (low intensity areas are surrounded by higher intensity areas), we employ a radial reach filter (RRF) [13]. RRF scans intensity profiles radially from a voxel of interest on a cross section. If a voxel currently being checked does not satisfy given conditions in the scan for a certain direction, we visit neighboring voxel along the direction. This process is iterated until we encounter a voxel satisfying the conditions. If the voxels found in all scans form a pre-defined shape (in our case, circular shape), the pixel of interest is extracted.

We apply the RRF by changing the normal of a cross section for each candidate voxel extracted in 2.3. If a voxel \mathbf{p} does not satisfy any of following four conditions,

- Condition (1) $f(\mathbf{p}) < T_1$,
- Condition (2) $f(\mathbf{s}_k) - f(\mathbf{p}) > T_2$ ($k = 1, 2, \dots, D$),
- Condition (3) More than $T_D\%$ of all scans satisfies the condition (2),
- Condition (4) $V[l_k] < T_V$,

the voxel \mathbf{p} is removed from candidate voxel set. In these conditions $f(\mathbf{p})$ is the intensity at a voxel \mathbf{p} . \mathbf{s}_k is the voxel satisfying the Condition (2) along a scan direction \mathbf{d}_k . The distance between \mathbf{s}_k and \mathbf{p} is represented by l_k . \mathbf{s}_k is then represented as $\mathbf{s}_k = \mathbf{p} + l_k \mathbf{d}_k$, where $\mathbf{d}_k = (\cos \psi, \sin \psi)^T$, $\psi = 2\pi(k-1)/D$, $l_k < L_{max}$, and D represents the number of scans. $V[x]$ denotes the variance of x . The Condition (1) checks whether $f(\mathbf{p})$ is sufficiently low as the bronchial lumen. The Conditions (2) and (3) decide whether \mathbf{p} is surrounded by higher intensity. Final Condition (4) checks whether higher intensity voxels surrounding \mathbf{p} forms the circular shape. The normal vector \mathbf{n} of a cross section whose $V[l_k]$ is minimum is estimated as the running direction of a bronchus at \mathbf{p} .

2.5 Postprocessing

The candidate voxels obtained so far include many false positives. Thus, we eliminate FPs as follows. First, we check whether two estimations of the running direction of a bronchus, \mathbf{c} and \mathbf{n} , are consistent by

$$\frac{|\mathbf{n} \cdot \mathbf{c}|}{\|\mathbf{n}\|\|\mathbf{c}\|} \geq T_a. \quad (5)$$

If a candidate voxel does not hold above equation, the voxel is removed from candidate voxel set. Then, a connected component whose number of voxels is less than T_c is removed as well. Since the bronchial candidates are detected at only central parts of bronchial tube structure, we recover the thickness of each tube based on estimated radius R . However, branching parts of thick tubes cannot be recovered well. Such parts may not be detected as bronchial tube structure because their shape on cross sections do not show circular one. Thus, by unifying the roughly extracted region by the simple region growing method [1] which extracts relatively thick branches up to subsegmental lobes at least and the recovered region, the bronchial region is finally extracted.

3 Experiments

We applied the proposed method to eight cases of 3D chest CT images. Specifications of the CT images are; 512×512 pixels in a slice, 209 - 751 slices in an image, 0.506 - 0.684 [mm] in pixel spacing, and 0.401-1.25 [mm] in slice spacing, respectively. We evaluated the extraction results by comparing with ground truth data which are generated manually by an author. The following three indices were used for evaluation: (a) Branch Detectability (BD) : percentage of the number of extracted branches out of bronchial branches manually detected, (b) True Positives (TP) : Number of extracted voxels which were true bronchial voxels, and (c) False Positives (FP) : Number of extracted voxels which were not bronchial voxels actually.

Parameters used in the experiment are shown in Table 1. They were set experimentally by searching adequate values one by one. Here, parameters for the tube extraction filter, T_2 , L_{max} , T_V and T_D , were gradually changed according to the estimated radius of a branch. Figures 2-4 and Table 2 show examples of the extracted bronchial regions and evaluated results by BD and FP in comparison with the previous (adaptive branch tracing) method [3]. In Figs. 2-4, ground truth data, TP and FP regions are shown in red, yellow and blue, respectively. As shown in Table 2, the number of extracted branches and BD by the proposed method are better than those by the adaptive branch tracing method, in particular, for Cases 7 and 8 which have a tumor inside the bronchial lumen. On the other hand, the amount of FPs of the proposed method increased relatively than that of the adaptive branch tracing method, though it reduced significantly in cases 1 and 3.

Table 1. Parameter setting used in the experiment.

σ	0.5	w	0.5 ($LoG(\mathbf{p}) \leq 0$)	T_i	250	T_a	0.9	T_c	500
			0.05 ($LoG(\mathbf{p}) > 0$)						
T_1	-700 [HU]	N	8	D	72				
$R > 10[mm]$			400 [HU]		R [mm]	2.0			100[%]
$R > 5[mm]$		T_2	250 [HU]	L_{max}	R [mm]	T_V	1.0	T_D	100[%]
$R > 3[mm]$			100 [HU]		5 [mm]		1.0		90[%]
otherwise			50 [HU]		5 [mm]		1.0		90[%]

Table 2. Comparison of results by the proposed and adaptive branch tracing (ABT) [3] methods. The term "BD" indicates the branch detectability.

Case	Number of branches	Number of extracted branches	BD of proposed method [%]	BD of ABT method [%] (Number of extracted branches)	FP of proposed method [mm^3]	FP of ABT method [mm^3]
1	385	260	67.5	69.9 (269)	1093.4	4883.2
2	331	229	69.2	63.7 (211)	2274.0	1575.7
3	422	323	76.5	55.7 (235)	3569.0	6609.4
4	490	409	83.5	75.5 (370)	16477.9	9101.3
5	236	142	60.2	46.6 (110)	402.3	230.9
6	511	322	63.0	65.6 (335)	1089.2	1615.5
7	171	126	73.7	23.4 (40)	1678.2	650.1
8	548	322	58.8	40.9 (224)	2203.5	629.7
ave	386.8	266.6	68.9	58.0(224.3)	3598.4	3162.0

4 Discussion

As shown in Figs. 2 and 3, the proposed method can extract bronchial regions beyond the interruption by a tumor. This is because our method detects candidate voxels which have bronchus-like intensity structure and select appropriate candidates from them, instead of tracing the bronchial tree as in previous methods [1, 3]. However, there are some FPs caused by other structure such as the esophagus and areas under furcation parts of blood vessels, because these FPs show partially similar intensity structure with the bronchial region. In particular for areas under furcation parts of blood vessels, since their intensity is slightly lower than lung parenchyma they seem to be surrounded by higher intensity objects. As the side effect of the sharpening operation, this intensity structure is emphasized as well. In Case 4, strong influence of the side effect causes large FPs. To reduce FPs more, we should take tree structural constraints into account in addition to our bronchus-like intensity structure measures. Utilization of a statistical bronchial atlas will give good constraints on our method. Adoption of algorithms based on global optimization such as a graph cut algorithm may also

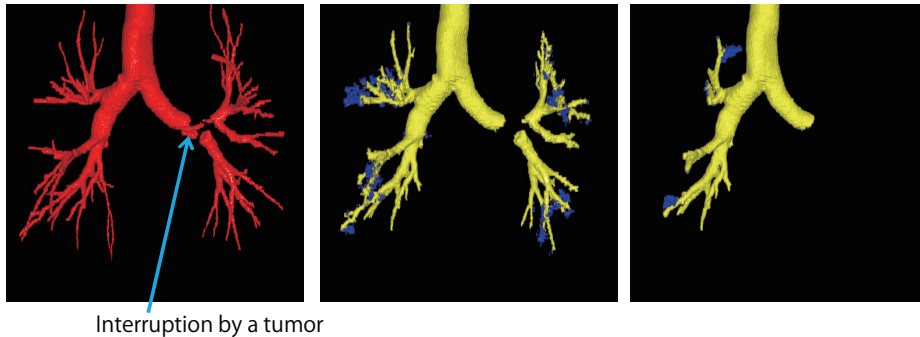


Fig. 2. Volume rendered results of the ground truth (left), the proposed method (middle) and the adaptive branch tracing method [3] (right) for Case 7. Yellow region indicates TP while blue region shows FP. Though the bronchial lumen is interrupted by a tumor indicated by arrow, the proposed method can extract the lumen regions beyond the tumor.

improve the accuracy of the proposed method. Furthermore, extraction parameter tuning, e.g. by machine learning approach, is one of future works since it also affects the accuracy of the proposed method.

5 Conclusions

This paper presented a method for extracting bronchial regions from 3D chest CT images by voxel classification based on local intensity structure. The proposed method detected candidate voxels which have bronchus-like intensity structure and selected appropriate candidates from them, instead of tracing the bronchial tree. The experimental results for eight cases of 3D chest CT images showed that the accuracy of the proposed method improved by 10 % compared with the adaptive branch tracing method, while FPs increased relatively. We also confirmed that the proposed method could extract bronchial regions beyond the interruption by a tumor.

References

1. K. Mori, J. Hasegawa, J. Toriwaki, H. Anno and K. Katada, "Automated Extraction and Visualization of Bronchus from 3D CT Images of Lung," Proc of 1st CVRMIed'95, pp. 542-548, 1995.
2. T. Kitasaka, K. Mori, J. Hasegawa and J. Toriwaki, "A Method for Extraction of Bronchus Regions from 3D Chest X-ray Images by Analyzing Structural Features of the Bronchus", *Forma*, vol.17, pp.321-338, 2002.
3. M. Feuerstein, T. Kitasaka and K. Mori, "Adaptive Branch Tracing and Image Sharpening for Airway Tree Extraction in 3-D Chest CT," Proc. of Second International Workshop on Pulmonary Image Analysis, ISBN: 978-1448680894, pp. 273-284, 2009.

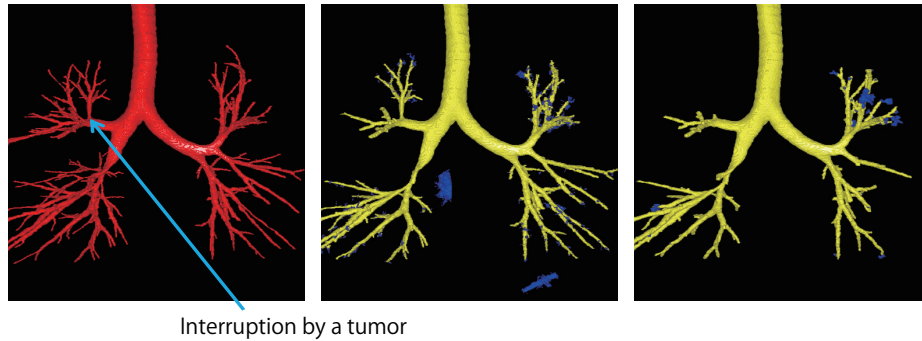


Fig. 3. Volume rendered results of the ground truth (left), the proposed method (middle) and the adaptive branch tracing method [3] (right) for Case 8. Yellow region indicates TP while blue region shows FP. Though the bronchial lumen is also interrupted by a tumor indicated by arrow, the proposed method can extract the lumen regions beyond the tumor.

4. J. Tschirren, E. A. Hoffman, G. McLennan and M. Sonka, "Intrathoracic airway trees: segmentation and airway morphology analysis from low-dose CT scans", *IEEE Transactions on Medical Imaging*, vol.24, no.12, pp.1529-1539, 2005.
5. T. Schlathoelter, C. Lorenz, I. C. Carlseña, S. Renischa and T. Deschamps, "Simultaneous segmentation and tree reconstruction of the airways for virtual bronchoscopy", *Proc. of SPIE on Medical Imaging*, vol.4684, pp.103-113, 2002.
6. P. Lo and M. de Bruijnea, "Voxel classification based airway tree segmentation", *Proc. of SPIE on Medical Imaging*, vol.6914, pp.69141K-1-12, 2008.
7. D. Aykac, E. A. Hoffman, Member, G. McLennan and J. M. Reinhardt, S. Member, "Segmentation and Analysis of the Human Airway Tree From Three-Dimensional X-Ray CT Images", *IEEE Transactions on Medical Imaging*, vol.22, no.8, pp.940-950, 2003.
8. A. Szymczak, A. Stillman and A. Tannenbaum, "3D Models of Airway Trees from CT Scans: A Point-Based Approach", <http://www.mines.edu/aszymcza/>
9. C. Bauer, H. Bischof and R. Beichel, "Segmentation of Airways Based on Gradient Vector Flow", *Proc. of Second International Workshop on Pulmonary Image Analysis*, pp.192-201, 2009.
10. C. Bauer, T. Pock, H. Bischof and R. Beichel, "Airway Tree Reconstruction Based on Tube Detection", *Proc. of Second International Workshop on Pulmonary Image Analysis*, pp.203-213, 2009.
11. P. Lo, J. Sporning, H. Ashraf, J. JH. Pedersen and M. de Bruijne, "Vessel-guided airway tree segmentation: A voxel classification approach", *Medical Image Analysis*, vol. 14, pp. 527-538, 2010.
12. Y. Sato, C. F. Westin, A. Bhalerao, S. Nakajima, N. Shiraga, S. Tamura and R. Kikinis, "Tissue classification based on 3D local intensity structures for volume rendering", *IEEE Transactions on Visualization and Computer Graphics*, vol.6, no.2, pp. 160-180, 2000.
13. Y. Sato, S. Kaneko, Y. Niwa and K. Yamamoto, "Robust object detection using a radial reach filter (RRF)", *Systems and Computers in Japan*, vol. 35, no. 10, pp. 63-73, 2004.

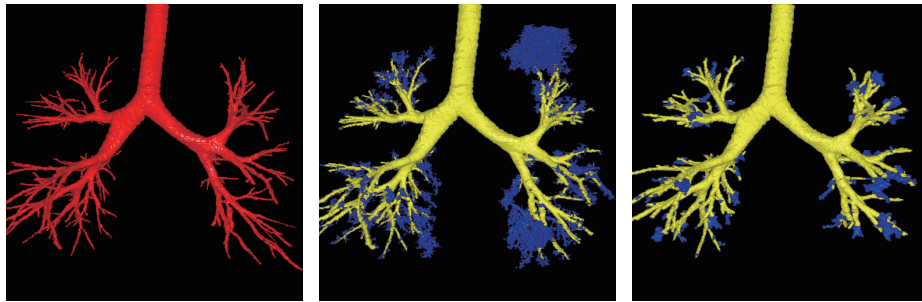


Fig. 4. Volume rendered results of the ground truth (left), the proposed method (middle) and the adaptive branch tracing method [3] (right) for Case 4. Yellow region indicates TP while blue region shows FP. The proposed method produced larger volume of FP than the adaptive branch tracing method, although BD became much better.